dam world 2018 Third International Dam World Conference
BRAZIL • Foz do Iguaçu • September 17-21, 2018

UPDATING OF THE BEHAVIOUR ANALYSIS AND INTERPRETATION OF CAHORA BASSA DAM (MOZAMBIQUE) CONSIDERING THE MID-BOTTOM SPILLWAY STRUCTURES

António L. Batista[*], Ivo F. Dias[*], José P. Gomes[*],
Ezequiel F. Carvalho[†], and Ilídio M. Tembe[†]

[*] Laboratório Nacional de Engenharia Civil (LNEC)
Av. do Brasil, 101, 1700-066 Lisboa, Portugal
e-mail: a.l.batista@lnec.pt

Keywords: Cahora-Bassa dam, Structural modelling, Monitoring, Alkali-aggregate reactions, Finite element method

Abstract. *This paper presents the updating of the behaviour analysis and interpretation of Cahora Bassa dam, a 166 m high double-curvature arch dam, located in the Zambezi river (Mozambique). The structural numerical model includes, in addition to the dam's body with the mid-bottom spillway holes, already considered in the previous studies, the downstream structures of that spillway.*

The results computed with the updated structural model together with the data provided by the dam monitoring system, support the analysis and interpretation of the dam behaviour, since the first filling of the reservoir, occurred in 1974, up to the end of 2016.

The structural model, based in 3D finite elements of the dam and its foundations, takes into account the concrete viscoelastic behaviour, the variation of the reservoir level and the expansions due to the moderate alkali-aggregate reactions (AAR) on the dam´s concrete.

The monitoring and the numerical results display an excellent agreement, showing the suitability of the finite element model for modelling the dam's behaviour. Additionally, the obtained results confirm the relevance and influence of creep and swelling effects in the dam structural response. Relatively to the stress fields, the computed results show that at the arch bearings the stresses assume already significant values.

The displacements computed at the mid-bottom spillway structures are important data for verifying the operation of the gates.

1 INTRODUCTION

The Cahora Bassa hydroelectric scheme, in which the dam is integrated, is located on the Zambezi river, close to Songo Village, Tete province, Mozambique.

The scheme mainly consists of the dam, the underground powerhouse, excavated in the rock mass of the right bank, which includes the water intakes and the penstocks upstream, as well as the surge chambers and the tailrace tunnels downstream. The installed capacity is of 2075 MW, divided by 5 ground power units of 415 MW / 480 MVA each. During the project development a second powerhouse was contemplated, on

[†] Hidroeléctrica de Cahora Bassa (HCB), Songo, Mozambique

the left bank (north), also underground, which was intended to be built in a 2nd stage (Figure 1).

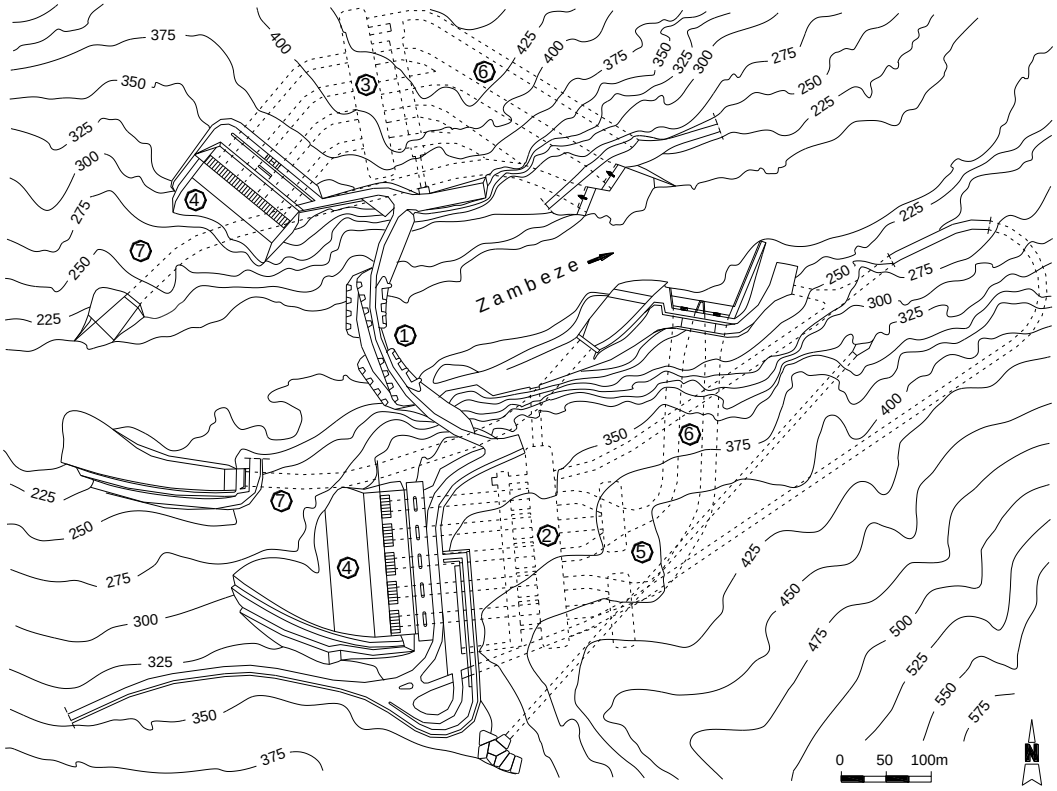

1 – Dam
2 – Southern powerhouse
3 – Northern powerhouse (to be built in a 2nd stage)
4 – Water intakes and penstocks
5 – Surge chambers
6 – Tailrace tunnels
7 – Diversion tunnels

Figure 1: General plan of the Cahora Bassa scheme

The rock mass, on which the scheme is installed, is of very good quality and mainly consists of gneissic granite. The rocks are sound and the rock mass is poorly fragmented. There are a few lamprophyre and gabbric veins, some of which were subject to specific treatment during construction.

The concrete dam is a double curvature arch dam with a 166 m maximum height, from the bottom level of the foundation. The crest is 303 m long, having a chord/height ratio of 1.54 and a thickness ranging, in the main cantilever, from 4 m at the crest to 23 m at the base. The crest and the retention water level (RWL) are located at levels 331.00 m and 326.00 m, respectively. The dam is equipped with a small surface spillway, of the "volet" type, and a mid-bottom spillway with 8 orifices (Figure 2).

The reservoir has a volume of about 66000 hm^3. The maximum discharge capacities of the surface spillway and of each spillway orifice are 600 m^3/s and 1600 m^3/s, respectively, amounting to a total discharge capacity of 13400 m^3/s.

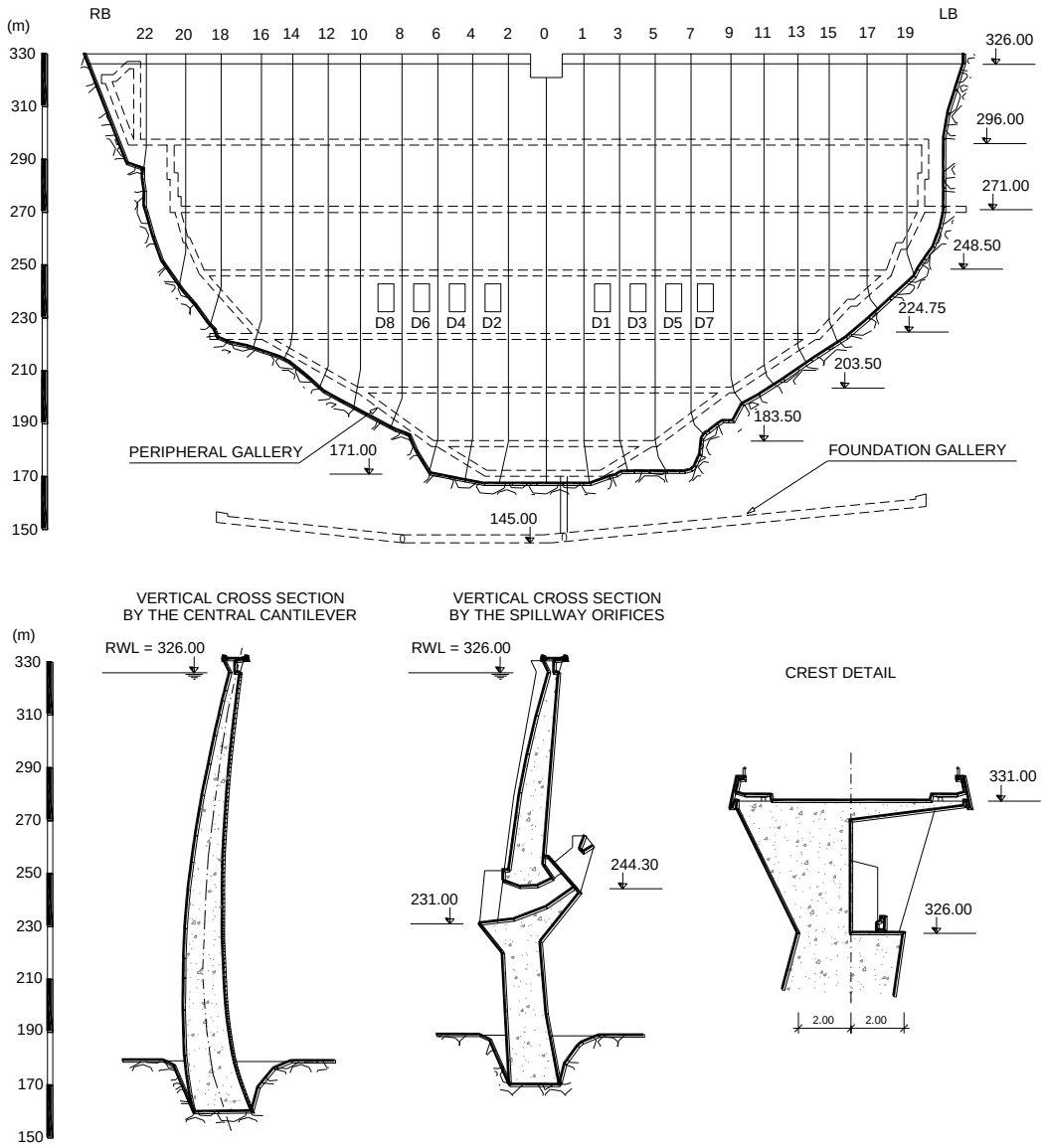

Figure 2: Cahora Bassa dam. Downstream elevation, vertical cross-sections and crest detail

The dam monitoring system allows the evaluation of the actions and the determination of the structural and hydraulic responses, by measuring: i) the upstream and downstream levels, by staff gauges and water level recorders; ii) air temperatures, by both thermometers and thermograph; iii) uplifts, by simple piezometers and by piezometer fans; iv) horizontal displacements, by coordimeter bases installed at the intersection of the five plumb lines with the inspection galleries; v) horizontal displacements by geodetic methods; vi) vertical displacements, by precision geometric leveling in some galleries, and by rod extensometers installed at the central cantilever of the dam and at the foundation, from the peripheral gallery; vii) convergences, by convergence meters installed close to the spillway orifices; viii) joint movements, using devices for measuring the movement of joints and deformeters; ix) temperatures in the concrete, by thermometers, by devices for measuring the movement of joints, by strain meters and stress meters; x) strains, by groups of two, five or nine Carlson strain meters; xi) stress, by stress meters; and xii) discharged and infiltrated flows, by drains and seepage measuring weirs. The dam is also equipped with a rain gauge, for measuring

rainfall, as well as with an earthquake monitoring system and a dynamic response monitoring system, formed by a seismometer network.

2 STRUCTURAL MODEL

2.1 Structural finite element model

A homogeneous continuous structural finite element model was used to support the interpretation of the dam behaviour. The continuous model is suitable for the analysis because of the very small movements occurring at the contraction joints since the first filling, which in turn are related to the small variations of the main loads (water level and thermal effects) and also to the concrete swelling, that contributes for closing the dam joints.

The concrete rheological behaviour was simulated by using a viscoelastic model, characterized by the creep function (1) and a Poisson ratio ν_c=0.2. For the rock mass foundation, also considered homogeneous and continuous, the time effects were not considered, being used a Young's modulus E_f=50.0 GPa and a Poisson ratio ν_f=0.2.

From creep tests performed at LNEC[1], information about the concrete composition, swelling quantification (calculated in previous studies by retro-analysis techniques[2]) and structural modelling[3,4], the following Bazant e Panula was predicted for the dam concrete,

$$J(t,t_0) = \frac{1}{50.0}\left(1 + 3.0(t_0^{-0.34} + 0.042)(t - t_0)^{0.18}\right) \qquad (\text{GPa}^{-1}) \qquad (1)$$

which is represented in Figure 3 for three ages of loading, as well as the corresponding relaxation curves obtained through numerical inversion. Mention must be made for the fact that the concrete presents considerable creep rates for high load ages, which also corresponds to a good stress relaxation capacity for prescribed strains.

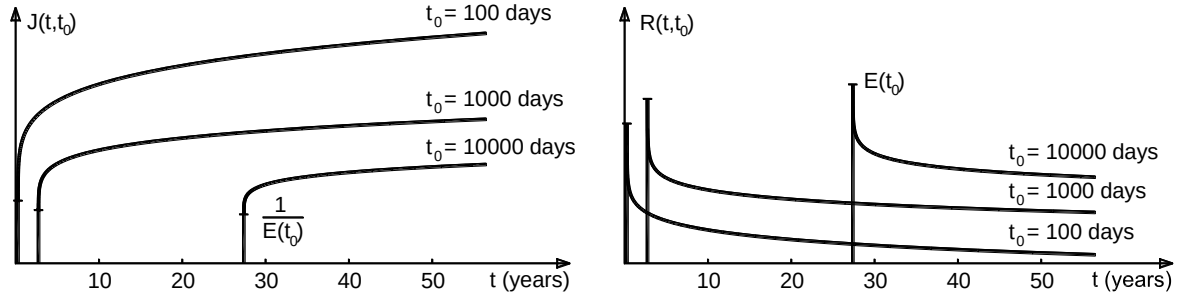

Figure 3: Creep and relaxation curves of Cahora Bassa dam's concrete

Relatively to the previous study of behaviour analysis and interpretation[5,6], the upgraded finite element mesh includes the foundation and the mid-bottom spillway structures. Additionally, it includes two elements in the thickness, which allows a better representation of the dam's crest geometry.

The finite element mesh (Figures 4 and 5) has a total of 6744 nodal points for 1176 volumetric 20-node hexahedral finite elements, from which 364 belong to the dam's body, 56 to the mid-bottom spillway structures and 756 to the rock mass foundation.

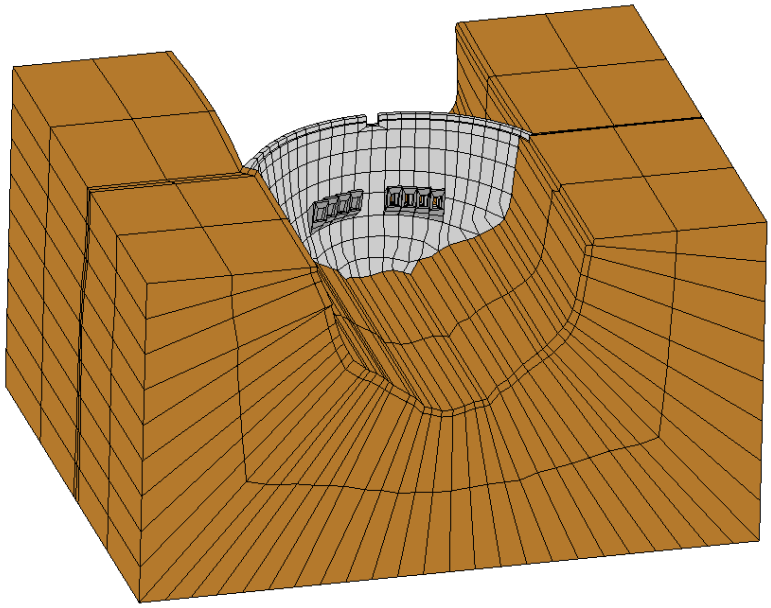

Figure 4: Downstream view of the finite element mesh of the dam and its rock mass foundation

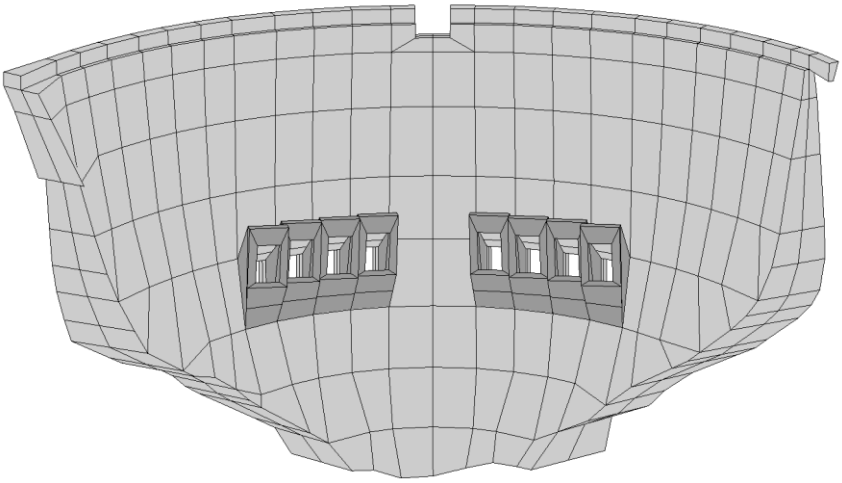

Figure 5: Downstream view of the finite element mesh of the dam and the mid-bottom spillway structures

2.2 Loads

For analysing the dam behaviour, from the beginning of the first filling to the end of 2016, the following loads were discretized in time and applied to the structural model: i) the concrete dead weight; ii) the prestressing forces in the spillway structures; iii) the hydrostatic pressure; iv) the temperature variations due to the annual waves in the air and in the reservoir; and v) the concrete swelling due to alkali-aggregate reactions.

The dead weight of concrete was represented by means of vertical body forces (γ_c=24 kN/m^3), the water pressure (

Figure 6) by surface loads, applied to the upstream surface of the dam and to the spillway gates (γ_w=10 kN/m^3), and the prestressing forces by punctual loads in the mesh nodes corresponding to tendons anchorages and deviations (Figure 7).

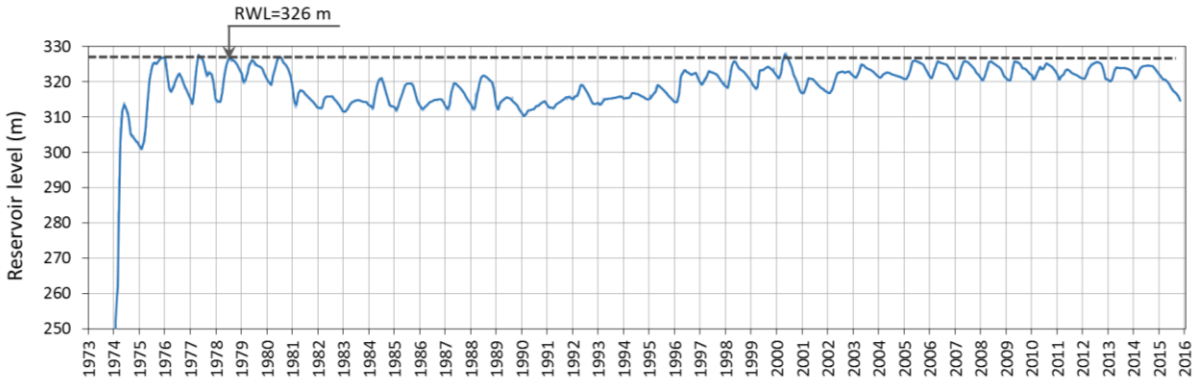

Figure 6: Monthly discretization of the reservoir level

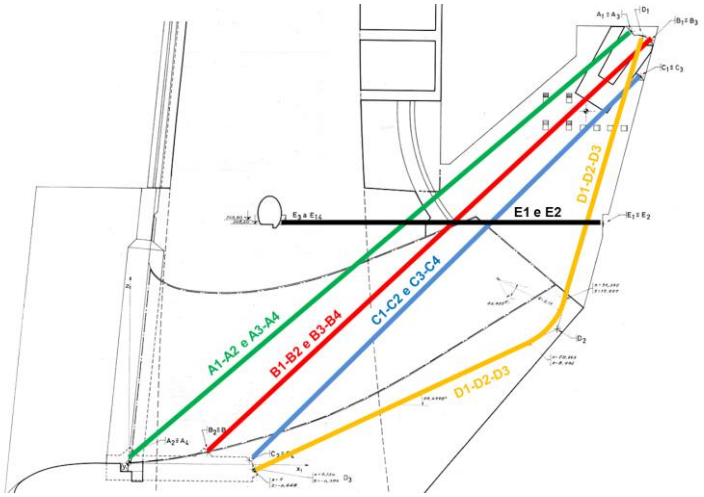

Figure 7: Prestressing tendons connecting the spillway structures to the dam's body (adapted from the design drawing nº 18408-B)

The thermal actions on the dam surfaces were represented by sinusoidal waves of annual period for the air and water. The wave parameters were numerically determined by the least square method based on the temperatures observed on air and water thermometers (Figure 8). For the concrete thermal dilation coefficient was considered a value of $\alpha=1.0\text{x}10^{-5}$ /ºC.

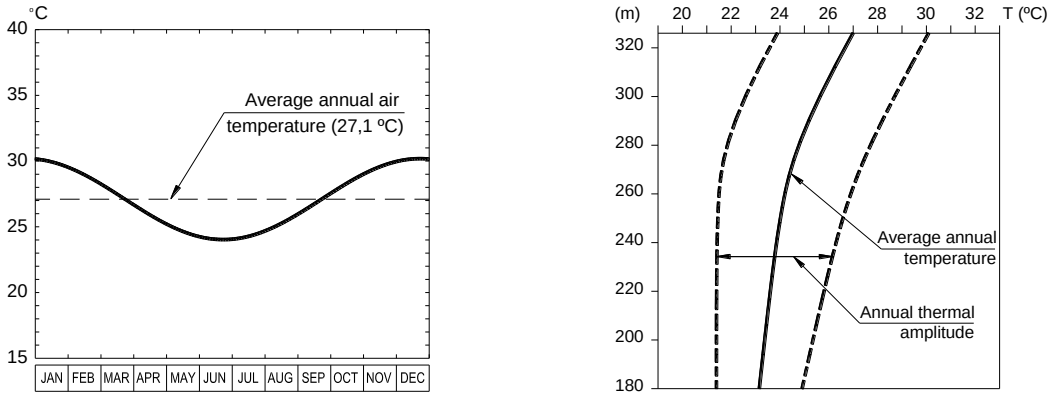

Figure 8: Average annual thermal wave on air and variation with depth of the average annual thermal wave amplitude of the reservoir water, evaluated from the monitoring data

The action of the concrete expansion was represented by means of imposed free-swelling deformations. The evolution of the concrete free-swelling in four different zones (Figure 9) was estimated on the basis of the information about the concrete composition (in particular the quantity of cement and alkali), the analysis of data from chemical studies, observations at stress free strain meters and geometric levelling, and also from results obtained with the numerical modelling[7].

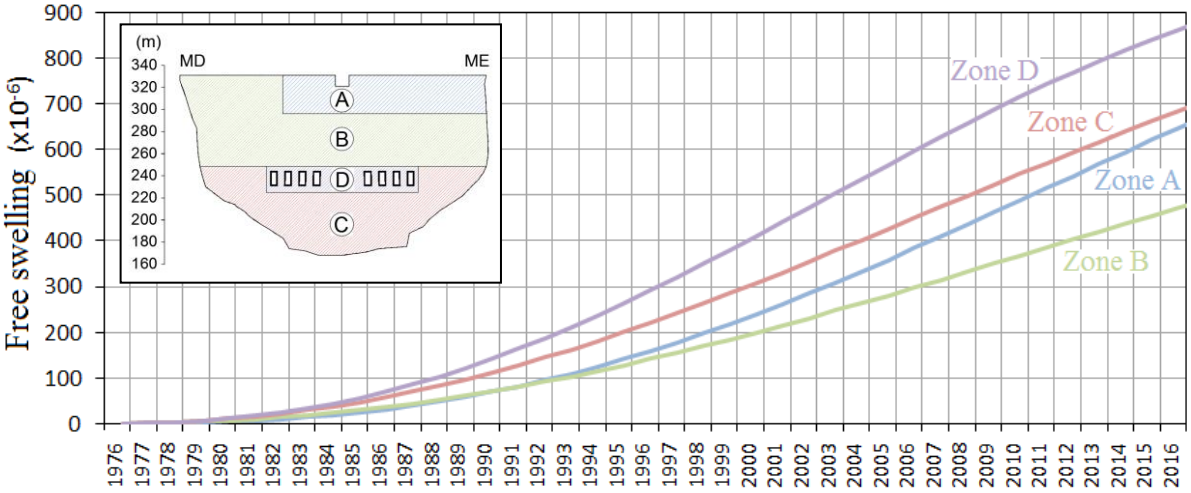

Figure 9: Zoning and evolution over time of free swelling strains in dam's body

The influence of stress field on swelling evolution was taken into account according the relation proposed by Larive[8] based on experimental studies (Figure 10), while changes on the concrete rheological behaviour were not considered since the swelling magnitude is still moderate.

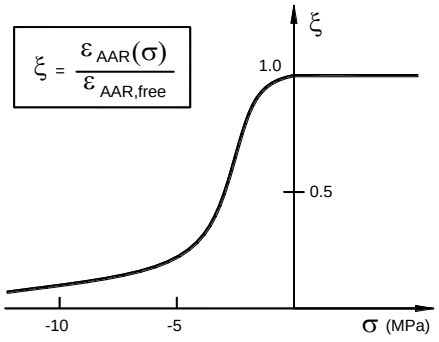

Figure 10: Relationship considered for taking into account the influence of the stress field on the swelling development

3 Analysis and interpretation of the structural behaviour

3.1 Arch dam structural response

The results computed by the structural model, together with the data provided by the dam monitoring system, support the analysis and interpretation of the dam behaviour.

Figure 11 shows the evolution of the radial displacements over time, observed in the central plumb-line at elevation 296.0 m, along with the values computed with the numerical model, considering the combined load of the dead weight, water pressure, swelling and their delayed effects. The good agreement between the computed and observed results is remarkable. The computed response is also depicted in the third plot

of the same figure, but there the effects are separately represented, so the relative weight of each effect can be appreciated. The delayed response is higher than the elastic response while the swelling effects start assuming relevant values. The elastic response is consistent with the evolution of the reservoir level, shown in the first plot of Figure 11.

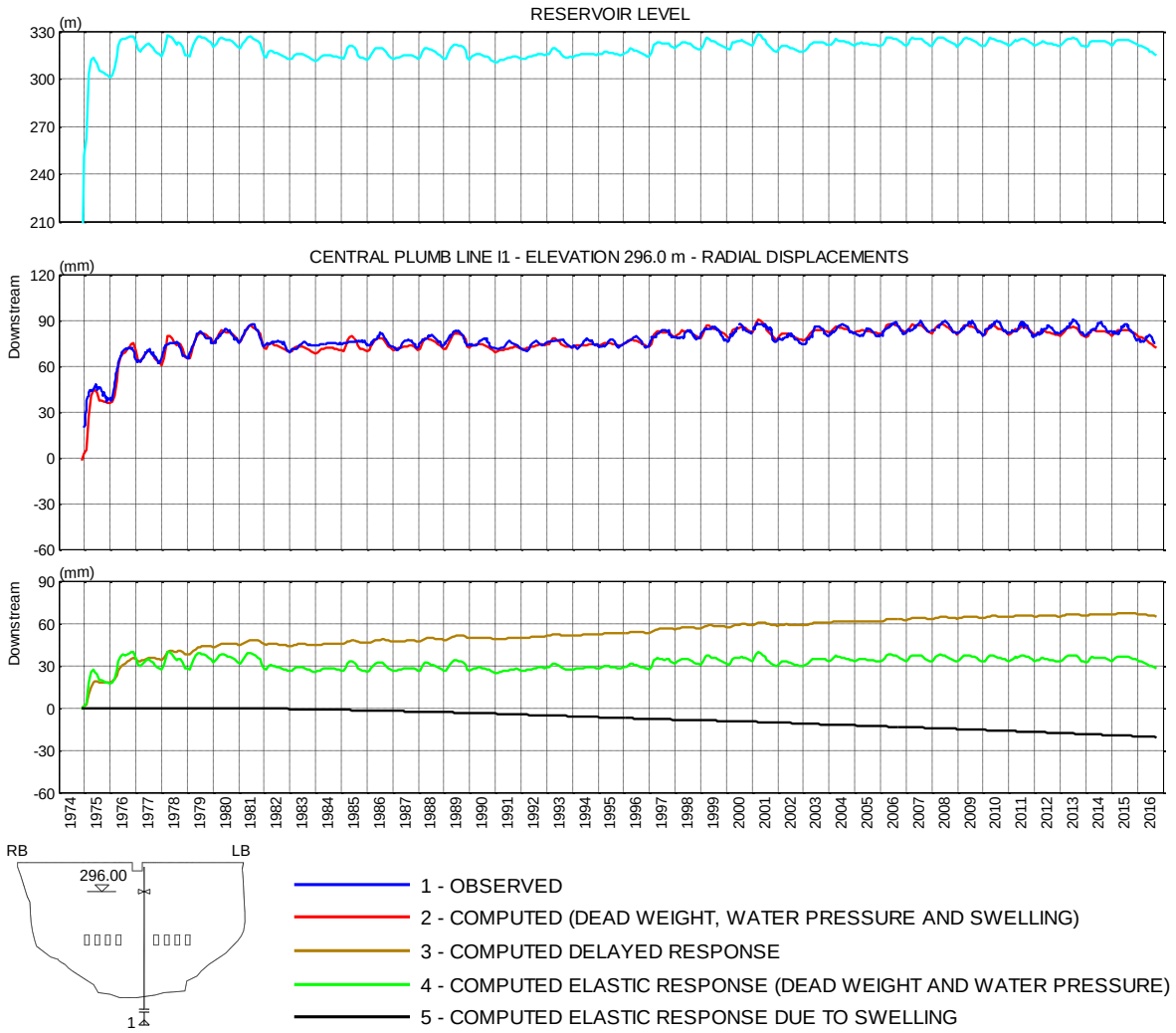

Figure 11: Central cantilever radial displacements at 296.0 m elevation, measured on the plumb line and computed, between 1975 and 2016

Figure 12 presents the evolution of the vertical displacement in a point corresponding to the levelling mark N14 of the gallery at elevation 326.0 m. The plots have an organization similar of Figure 11, omitting the evolution of the reservoir water level. The first plot shows that the computed vertical displacements compare well with those observed by the geometric levelling. The second plot, where the effects are separately represented, shows that the vertical displacements is almost entirely due to swelling effects.

FFigure 13 presents a comparison of deflection curves corresponding to the computed vertical displacements and those observed by geodetic levelling in the gallery of the dam at 326.0 m elevation, between July 1977 and July 2016. The plot shows the good agreement between both curves.

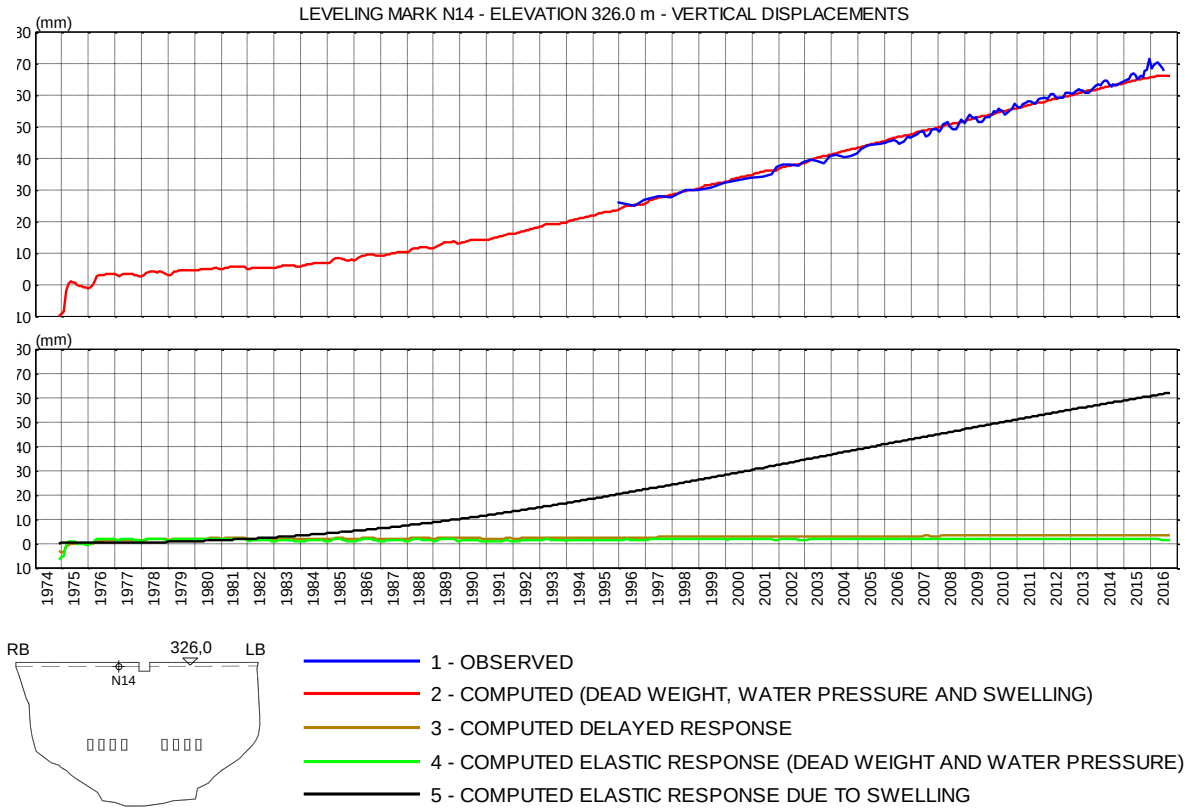

Figure 12: Vertical displacements at 326.0 m elevation, at a point corresponding to the levelling mark N14, computed and measured by geometric levelling, between 1975 and 2016

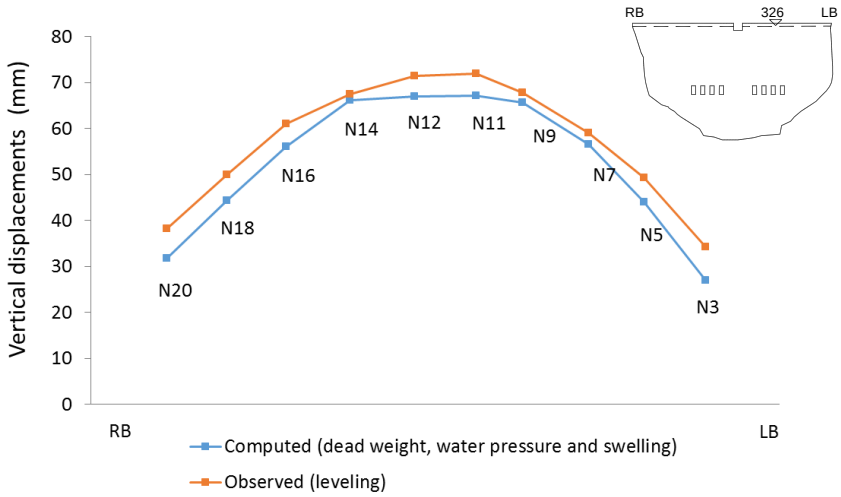

Figure 13: Vertical displacements at 326.0 m elevation gallery observed and computed between July 1977 and July 2016

Figure 14 presents the horizontal strains evolution at a point corresponding to the single extensometer number 35, located 1 m from the upstream surface, at elevation 244.85 m, above the two central spillway orifices, on the right bank side. The observed values are compared with those computed with the numerical model. For this case, it is also noticed the excellent agreement between the monitoring and the computed results. Mention must be made to the fact that the strains observed and calculated above the spillway orifices

have a progressive increase over time, with accumulated values, between 1976 and 2016, of about -200x10^{-6}.

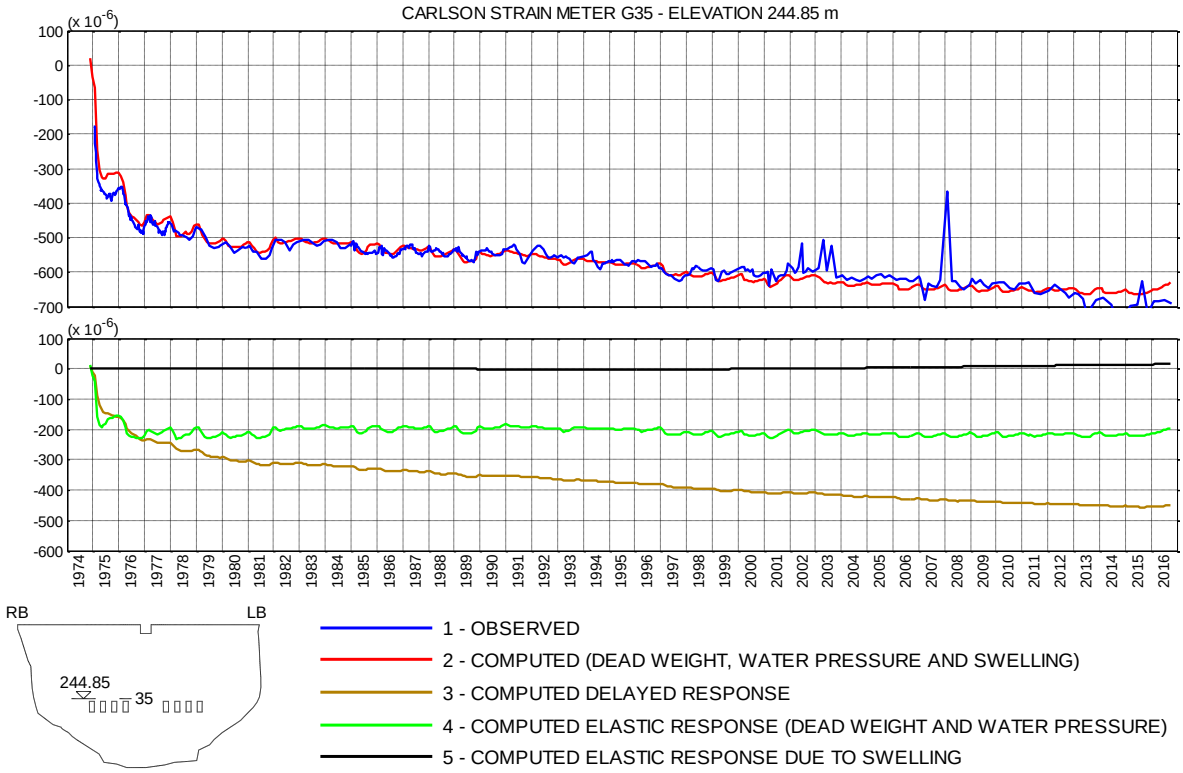

Figure 14: Horizontal strains of the point corresponding to the Carlson strain meter G35, at elevation 244.85 m (upstream), observed and computed between 1975 and 2016

The left hand side of Figure 15 presents the principal stresses on the upstream and downstream surfaces, calculated at the end of 2016, with the reservoir water at level 314.7 m, due to the combined loads of the dead weight, hydrostatic pressure and swelling, as well as their delayed effects. The stress field is generally compressive except for the upper part of downstream surface, where tensile stresses occur. In compression, the maximum values reach 21 MPa and 17 MPa at the upstream and downstream surfaces of the left bank bearing, respectively. At the closure of the arches, above the spillway orifices, the maximum compressive stresses are about 11 MPa, downstream. The tensile stresses are vertical and lower than 1.5 MPa at the closure of the upper arches, and diagonal and superior to 1.5 MPa near the bearings, with values reaching 4 MPa in some localized zones.

The right hand side of Figure 15 presents the principal stresses on the upstream and downstream surfaces calculated at the end of 2016, due to swelling and corresponding delayed effects, in particular relaxation. Stresses with significant values appear along the dam insertion. The higher compressive stresses are located at the bearings of the upper arches, reaching values of about 20 MPa at the left bank, upstream, while the higher tensile stresses, of about 4 MPa, are found downstream with orientation fairly normal to the foundation insertion surface.

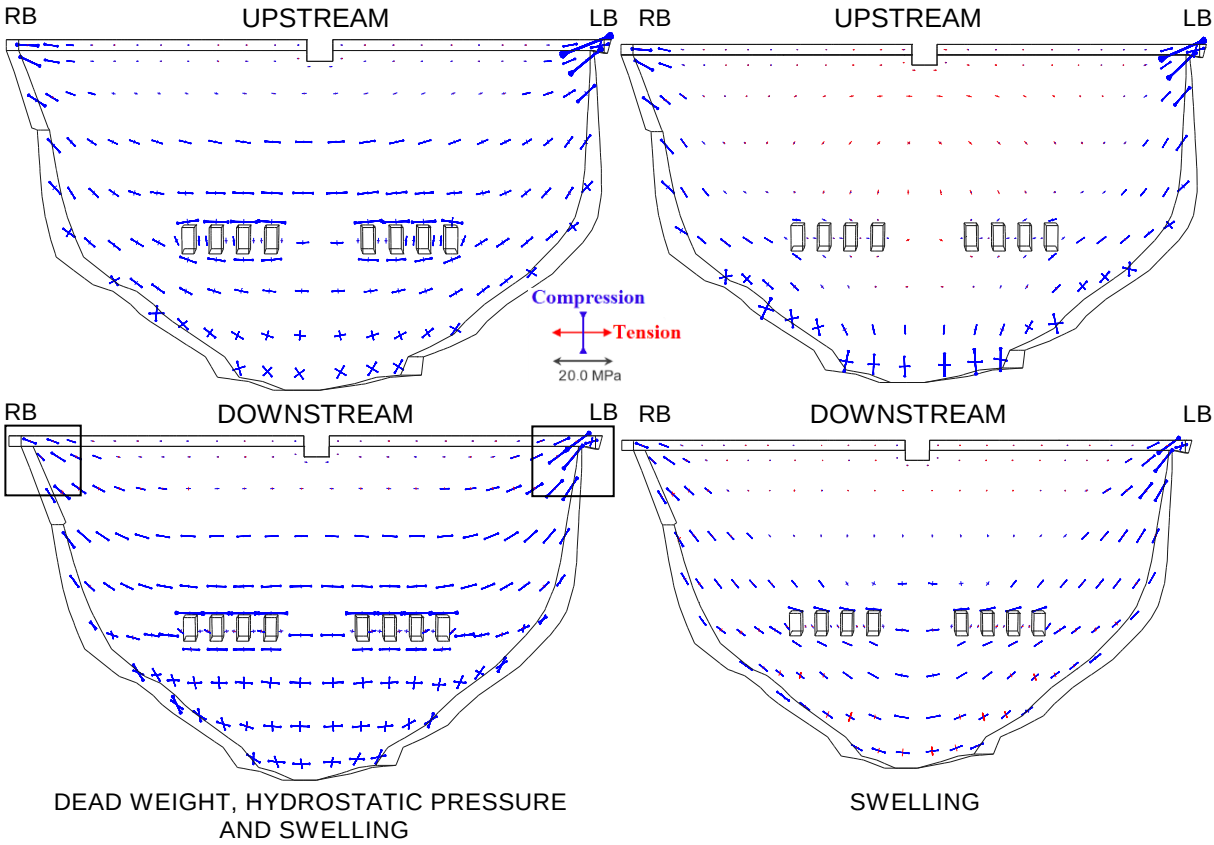

Figure 15: Principal stresses on dam surfaces computed at the end of 2016, due to the combined loads of the dead weight, hydrostatic pressure and swelling (left side) and only due to swelling (right side)

Figure 16 shows a detail of the stress field at the upper arches near the bearings (zones inside the rectangles marked on Figure 15). At the left bank, in the zone connecting the open gallery, at the elevation 326 m, with the left bank access, diagonal tensile stresses of about 4.0 MPa take place, justifying the cracks in the dam surface and as well their dominant direction. In the right bank, there are also tensile stress of about 4.0 MPa in the zone corresponding to the beginning of the bearing enlargement, which also justify the cracks found in this zone.

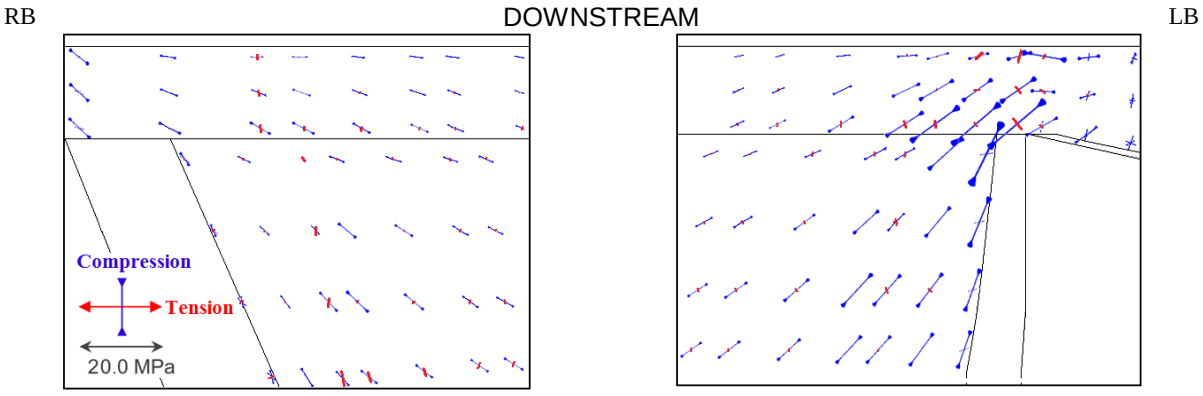

Figure 16: Detail of the stress field at the downstream surface of the upper arches near the bearings at the end of 2016, due to the combined loads of the dead weight, hydrostatic pressure and swelling

The daily thermal variations registered in the downstream surface thermometer are about 10ºC[5], causing, near the surface, alternating compressive and tensile stresses. By considering a plane stress approximation with instantaneous elastic modulus of E_c=42.5 GPa and Poisson ratio of ν_c=0.2, that is, discarding the relaxation effects, the daily stress variations are of about,

$$\Delta\sigma = \frac{E}{1-\nu}\alpha\Delta T\frac{42.5\times10^{6}}{1-0,2}\times1.0\times10^{-5}\times5.0 = 2660\ \text{kN/m}^2 = 2.7\ \text{MPa} \quad (2)$$

that should be added to the values of Figures 15 and 16, so the maximum compressive stress downstream became about 20 MPa at the bearings and the maximum tensile stress reach about 6.7 MPa, also downstream.

3.2 Spillway structures response

The convergences of the spillway structures were measured in between the vertical interior surfaces of the structures, close to the orifices, from 1994 to 2004. After an interruption period the observations were restarted in 2011 for the orifices 1, 2 and 4.

Figure 17 plots the relative displacements in between the spillway structures, corresponding to the first orifice, showing that the swelling effect contributes for the progressive approximation of the lateral surfaces of the mid-bottom spillway orifices.

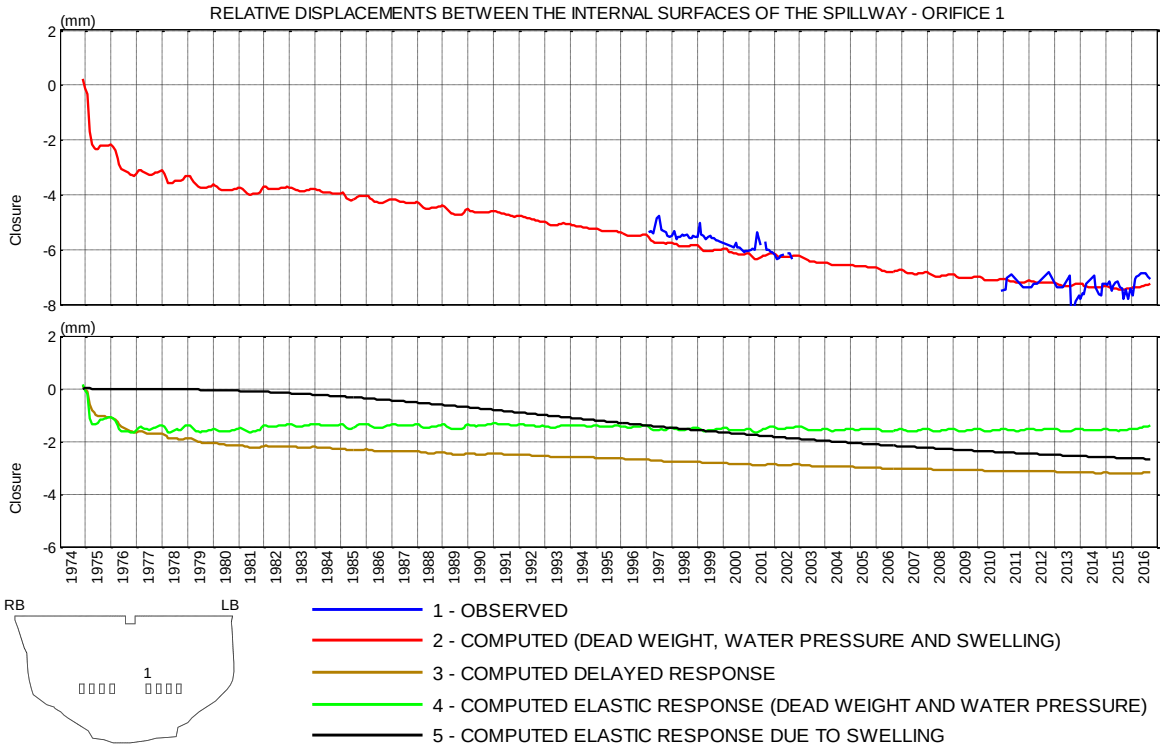

Figure 17: Relative displacements between the internal surfaces of the spillway structures, corresponding to the first orifice of the mid-bottom spillway, computed between 1975 and 2016 and observed between 1994 and 2002 and between 2011 and 2016

Figures 18 and 19 show, respectively, the principal stresses at the chute slab and lateral walls of the mid-bottom spillway structures, due to the combined loads of the dead weight, hydrostatic pressure in the upstream surface of the dam and at the spillway gate, prestressing, swelling and the delayed effects of this set of actions.

For the slab, the higher compressive stresses occur at the upper part of the zone connecting the slab to the dam's body, with values of about 7.0 MPa, while the higher tensile stresses, of about 3.5 MPa, occur in the opposite extreme of the slab, in the zones connected with the lateral walls. For the lateral walls, the higher compression stresses are of about 9.0 MPa, occurring in the external surface of the wall, at the bottom part of the zone connecting the wall to the dam's body and the higher tensile stresses reach 3 MPa at the top of the external surface and at the intermediate part of the internal surface.

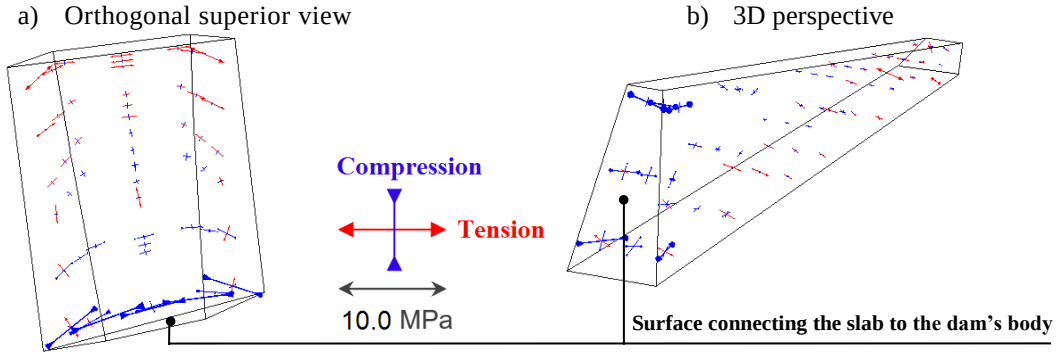

Figure 18: Principal stresses at the spillway slab (corresponding to the first orifice) computed by the end of 2016 with reservoir at level 314.7 m: a) orthogonal superior view and b) 3D perspective

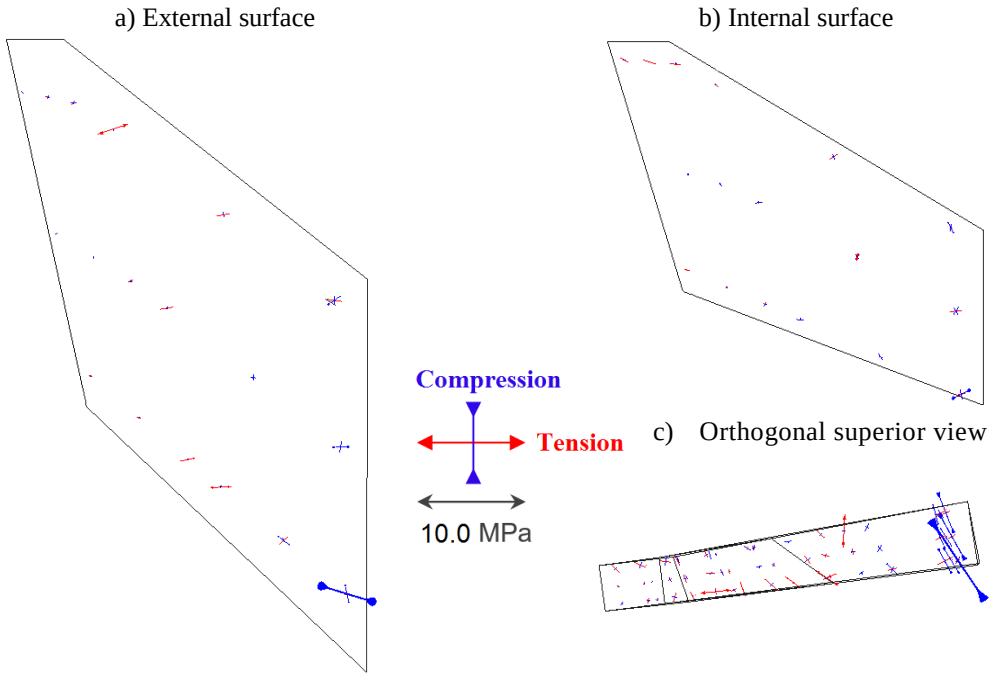

Figure 19: Principal stresses at the spillway lateral walls (first orifice), computed by the end of 2016 with reservoir at level 314.7 m: a) external surface; b) internal surface and c) orthogonal superior view

4 CONCLUSIONS

The mathematical methodologies used for interpreting the structural behaviour of Cahora Bassa dam over time have proven to be adequate, having into consideration both the instantaneous and the delayed effects of the main loads acting in the dam: dead weight, hydrostatic pressure, temperature variations and concrete swelling.

The creep function, adjusted in previous studies, remain modelling adequately the concrete behaviour, allowing an accurate prediction of the delayed structural response and the swelling development. Besides, the remarkable agreement between the observed and calculated results, in terms of either displacements or strains, gives reliability to the conclusions drawn from the numerical analysis.

The behaviour analysis of the dam shows that the swelling has led to the increase of compressive stresses on a large part of the dam and to a decrease along the insertion, downstream, and on the upper central zone, upstream. Due only to swelling, the compressive stresses reach values of about 20 MPa at the bearing, in the left bank, upstream, whereas the highest tensions reach values of about 4 MPa, near the insertion

surface, downstream. In fact, at the current date the compressive stresses due to dead weight and hydrostatic pressure cancel these tensile stresses.

By considering the combination of all loads, the resulting stress field is generally compressive, except for the upper part of downstream surface, where tensile stresses occur. The peak of compression stresses reaches 21 MPa at the upstream surface of the left bank bearing, and 11 MPa at the closure of the arches above the spillway orifices. At the bearings, the compressive stresses assume already significant values, but should be remarked that the mean value of the structural concrete strength is 61.6 MPa, thus the higher stresses are about 34% of the concrete capacity.

The tensile stresses are relevant only near the bearings, downstream, with the maximum values of about 4.0 MPa, to which the effects of the thermal variations, estimated around 2.7 MPa, should be added, totalizing 6.7 MPa. This value is higher than the mean tension strength (about 5 MPa) justifying the cracks existing in the zone.

At the mid-bottom spillway structures, the stress field is moderate, being computed for the combined service loads, maximum compressive stress values of about 9 MPa, at the zone connecting the structures to the dam's body and about 3.5 MPa maximum tensile stresses at the zone connecting lateral walls to the slab. At the transversal beam that supports the gate, the stresses are also moderate, being less than 2.0 MPa in tension.

The computations show a progressive approximation of the lateral surfaces of the mid-bottom spillway orifices, due to the concrete swelling. This issue, apparently, did not have affected the operability of these safety devices, since the gates are mounted in structures far from the dam's body. Nevertheless, the local behaviour of these zones should be properly monitored.

REFERENCES

[1] J.M. Ramos, *Consideration of the concrete rheology in the dam's behaviour (in Portuguese).* Specialist Thesis, LNEC, Lisbon (1985)

[2] A.T. Castro, A.L. Batista, J.M. Ramos, J.S. Pinho, *Parameter identification of a rheological model of the dam's concrete from prototype observation (in Portuguese).* 2º Encontro Nacional sobre a Análise Experimental de Tensões, Lisbon (1990)

[3] C. Larive, *Combined contribution of experimentation and modelling to the understanding of the alkali-reaction and its mechanical effects (in French).* PhD Thesis, Ecole Nationale des Ponts et Chaussées, Paris (1997)

[4] A.L. Batista,.C. Pina, J.M. Ramos, *Creep analysis of arch dams*. Technical paper nº 780, LNEC, Lisbon (1992)

[5] LNEC, *Cahora Bassa hydroelectric scheme - Dam behaviour analysis, interpretation and prevision.* Report 341/2009, LNEC, Lisbon (2009)

[6] A.L. Batista, J.P. Gomes, E.C. Fernandes, I.M. Tembe, *Analysis and interpretation of the structural behaviour of Cahora Bassa dam (Mozambique).* First International Dam World Conference, Maceió, Brazil (2012)

[7] LNEC, *Cahora Bassa dam - Updating of the interpretation analysis of the observed behaviour considering the mid-bottom spillway structures (in Portuguese).* Report 40/2017, LNEC, Lisbon (2017)

[8] LNEC, *Observation and analysis of the Cahora Bassa dam behaviour (1975-2001) (in Portuguese).* Report 178/02, Volumes I and II, LNEC, Lisbon (2002)